

Quantum Machine Learning for Robust Channel Estimation in Cyclic Prefix-Free OFDM Systems With Impulsive Noise

Caio N. Silva, Andrias M. M. Cordeiro, João T. Dias, Demerson N. Gonçalves, Tharso D. Fernandes

Abstract—Channel estimation in OFDM systems requires minimal complexity with one-tap equalizers and it is generally performed based on pilot symbols (PS) using least squares (LS). However, in a practical environment where impulsive noise may be present, this method may not be effective; furthermore, the minimal complexity required depends on cyclic prefixes (CP), which must be sufficiently large to cover the channel impulse response. In contrast, the use of PS and CP decreases the useful information that can be conveyed in an OFDM frame, thereby degrading the spectral efficiency of the system. In this context, we propose the use of quantum machine learning algorithms for channel estimation in OFDM systems with a reduced number of PS, without PS, and without CP. Our approach involves adapting classical machine learning models, specifically support vector regression and K-means clustering, to their quantum counterparts by integrating quantum kernels and encoding strategies suitable for channel modeling. The performance of the resulting quantum models is evaluated in comparison to LS and classical learning-based estimators. The viability of our approach is substantiated by computational simulation results obtained in frequency-selective channel models with the presence of non-Gaussian impulsive noise interfering with the symbols.

Index Terms—Channel estimation, OFDM systems, QML, QSVR, QK-Means, LS.

I. INTRODUCTION

ORTHOGONAL Frequency Division Multiplexing (OFDM) has emerged as a prominent scheme for high-bit-rate wireless networking standards [1]–[6]. Its primary advantage lies in its ability to eliminate intersymbol interference (ISI) and intercarrier interference (ICI) without requiring complex equalization filters at the receiver. While ISI is mitigated through the use of a cyclic prefix, ICI poses challenges in dynamic channels or when there are local oscillator mismatches with high carrier frequency offsets (CFOs). Common strategies to improve the useful data rate in OFDM systems include reducing the pilot

rate, increasing the number of subcarriers, or raising the modulation order. However, each approach introduces specific trade-offs. Reducing the pilot rate compromises the accuracy of channel estimation, making the system more vulnerable to rapid channel variations, frequency selectivity and noise. Increasing the number of subcarriers, while maintaining the same bandwidth to prevent adjacent channel interference, escalates both computational complexity and the required clock speed for signal processing. Lastly, adopting a higher modulation order degrades the bit error rate (BER) at the receiver.

In the context of the advancement of digital communication systems, Machine Learning (ML) has been widely employed to address complex problems [7]–[11]. Support Vector Regression (SVR) has demonstrated effectiveness in tackling challenges such as channel estimation in nonlinear environments [7], while unsupervised ML techniques like K-Means have been proposed to solve a variety of problems in digital communications [10], including channel estimation [11].

The integration of Quantum Machine Learning (QML) into modern communication networks has gained increasing attention due to its potential to enhance data processing, security, and network optimization. As 6G networks advance beyond their 5G predecessors, the incorporation of Quantum Computing (QC) is expected to play a crucial role, not only in areas such as Quantum Key Distribution (QKD) but also in enabling rapid data analysis and improved network efficiency through QML techniques [12]. The convergence of ML and quantum communication has already led to significant advancements, particularly in optimizing quantum protocols such as quantum key distribution, quantum teleportation, and quantum secret sharing, enabling more secure and efficient large-scale communication networks [13]. A key challenge in scaling up QML systems lies in the fragile nature of quantum processors. Despite this growing interest, several challenges still limit the practical adoption of QML in, for example, real-world wireless systems. Contemporary quantum processing units (QPUs) operate in the noisy intermediate-scale quantum (NISQ) regime, with limited qubit counts, short coherence times, and non-negligible gate noise, which constrain circuit depth and scalability. These limitations often push QML-based solutions toward remote or hybrid deployments, increasing latency and complicating real-time operation. In addition, variational QML models suffer from trainability issues such as barren plateaus and commonly rely on idealized data-

Caio N. Silva (ORCID: 0009-0000-9343-3304; e-mail: caio.silva.1@aluno.cefet-rj.br), Andrias M. M. Cordeiro (ORCID: 0009-0008-5868-6881; e-mail: andrias.cordeiro@aluno.cefet-rj.br), João T. Dias (ORCID: 0000-0001-9391-9830; e-mail: joao.dias@cefet-rj.br), Demerson N. Gonçalves (ORCID: 0000-0001-9130-7363; e-mail: demerson.goncalves@cefet-rj.br) are with Federal Center for Technological Education of Rio de Janeiro (CEFET/RJ) and Tharso D. Fernandes (ORCID: 0000-0003-3971-7394; e-mail: tharso.fernandes@ufes.br) is with Federal University of Espirito Santo (UFES).

This work was partially financed by the programs "GPESQ-CEFET/RJ", "PIBIC/CNPq" and "INOVA-CEFET/RJ – PIBITI/CNPq".

Submission: 2025-06-19, First decision: 2025-10-13, Acceptance: 2026-03-09, Publication: 2026-03-21.

Digital Object Identifier: 10.14209/jcis.2026.6

access assumptions (e.g., QRAM) that are not yet realizable in practice. Moreover, most QML-for-communications studies remain simulation-based, while SDR and testbed demonstrations, where latency and system integration challenges become evident, are still scarce. Consequently, further advances in algorithms, hardware, and system-level integration, including SDR-QPU prototyping and end-to-end latency evaluation, are required before QML can be reliably deployed in operational wireless networks [14]–[16]. However, recent developments in distributed quantum machine learning (DQML) propose integrating quantum processor units (QPUs) via classical communication, effectively mitigating hardware limitations while maintaining competitive classification accuracy [17]. This approach paves the way for scalable quantum-enhanced ML models, which can be deployed even on current intermediate-scale quantum processors. Additionally, the synergy between ML and quantum computing has opened new research avenues, particularly in error correction, quantum cryptography, and optimizing quantum network architectures [18]. Recent investigations have also expanded into adaptive modulation schemes to improve system performance. For instance, works such as [19] demonstrate that Quantum Fisher-preconditioning can stabilize learning in noisy environments for link adaptation, while [20] proposes intelligent architectures for optimizing channel selection and modulation in dynamic conditions.

These recent advancements underscore the growing relevance of QML in next-generation wireless communication systems, reinforcing the motivation for exploring Quantum Support Vector Regression (QSVR) and Quantum K-Means (QK-Means) for channel estimation in OFDM systems.

In this study, we propose the use of QSVR and QK-Means for channel estimation in an OFDM system without a CP, particularly in frequency-selective channels with the presence of impulsive noise. Our work aims to contribute to the field by integrating well-established quantum algorithms into a relevant and challenging telecommunications problem. The removal of the CP, while beneficial for spectral efficiency, introduces complexities that require robust estimation techniques. The integration of QSVR and QK-Means into this context represents a novel application of QML, leveraging quantum kernels and clustering to enhance channel estimation performance. Additionally, the experimental comparison with classical methods demonstrates that QSVR surpasses SVR in certain conditions, such as with 16-QAM modulation, indicating that QML methods can offer performance gains under specific scenarios. At the same time, the sensitivity of QK-Means to impulsive noise highlights the need for further exploration and refinement of quantum-based techniques for practical deployments. By addressing a critical issue in modern wireless communications and providing an experimentally validated assessment of QML methods, this study aligns with the ongoing efforts to enhance the efficiency and reliability of next-generation wireless systems. The presented results and discussions contribute to the growing body of research exploring the intersection of QC, ML, and telecommunications, reinforcing the relevance and potential impact of quantum-assisted solutions in real-world communication networks.

This article is organized as follows. Section II presents the

OFDM system modeling framework, describing the key components and signal representations used throughout the study. Section III presents the classical channel estimation methods, including LS, SVR and K-Means clustering, with emphasis on their formulation and limitations in noisy environments. Section IV presents the quantum-based methods for channel estimation. It includes a discussion of quantum kernels and Pauli-based feature maps, followed by the description of the proposed QSVR and QK-Means models. This section also presents a theoretical analysis of the computational complexity of classical and quantum models. Section V presents the simulation results and comparative analysis under various noise conditions and modulation schemes. Section VI concludes the paper and outlines possible directions for future research.

II. OFDM SYSTEM MODELING FRAMEWORK

A Single Input Single Output (SISO) scenario was considered in this study. The complete block diagram of the implemented OFDM system is shown in Fig. 1. The system was tested both with and without the addition of the cyclic prefix. Additionally, the channel estimators were placed in different positions: SVR and QSVR were applied in the time domain, as shown in the Fig. 1, while LS, K-Means, and QK-Means were positioned after the DFT. In this system, the input bits (b) are mapped into frequency domain symbols (s), which are then transformed into time domain samples (x). The received signal in the time domain is denoted by (y), while its corresponding frequency domain representation is (\hat{s}). Finally, the estimated bits after processing are denoted by (\hat{b}). These notations correspond to different stages of the OFDM transmission and reception process.

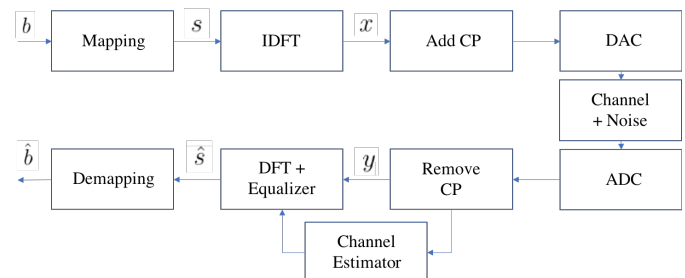


Fig. 1: Block diagram of the implemented OFDM system.

The OFDM signal can be expressed in the time domain by [1]

$$x[n] = \sum_{k=0}^{K-1} s_k e^{j2\pi \frac{k}{K} n}, \quad (1)$$

where s_k is the data symbol on the k -th subcarrier and K is the number of subcarriers in the OFDM symbol.

The signal at the receiver can be written by

$$y[n] = \sum_{k=0}^{K-1} s_k H_k e^{j2\pi \frac{k}{K} n} + \omega_n + b_n g_n, \quad (2)$$

where $y[n]$ is a time-domain sample before DFT transformation, H_k is the channel's frequency response at the k -th subcarrier and ω_n is an additive white Gaussian noise (AWGN), and

$b_n g_n$ is the impulse noise modeled as a Bernoulli–Gaussian process, i.e., the product of a real Bernoulli process b_n with $Pr(b_n = 1) = p$ and a complex Gaussian process g_n [21]. Then, residual noise at the receiver side is given by the sum of both terms $z_n = \omega_n + b_n g_n$.

III. CHANNEL ESTIMATION

Channel estimation can be performed in the time domain or the frequency domain and with or without the use of pilots. When using pilot symbols s_p , they are typically inserted between data symbols. These pilot symbols allow for the initial estimation of the channel's frequency response across a subset κ_p of subcarriers, known as pilot positions, with a cardinality $|\kappa_p|$. Then, the channel's frequency response is interpolated across the remaining $K - |\kappa_p|$ subcarriers. Therefore, the signal at the receiver can be rewritten as

$$y[n] = \sum_{k \in \kappa_p} s_p(k) H_p(k) e^{j2\pi \frac{k}{K} n} + e_n, \quad (3)$$

where, y represents the received signal in the time domain; $s_p(k)$ denotes the pilot symbol transmitted on the k -th subcarrier; $H_p(k)$ represents the frequency response of the channel at the k -th subcarrier and

$$e_n = \sum_{k \notin \kappa_p} s(k) H(k) e^{j2\pi \frac{k}{K} n} + z_n \quad (4)$$

covers residual noise and interference from non-pilot subcarrier data symbols. Here, these unknown symbols carrying information will be considered as noise for the time domain estimation methods. It is well known that for a channel impulse response with a maximum of L resolvable paths (and, consequently, degrees of freedom), then $|\kappa_p| \geq L$ [22].

For estimation without the use of pilots (blind estimation), the estimator must extract information about the channel from the data. In this case, the receiver knows the type of modulation applied to the data at the transmitter and estimates the phase and amplitude deviation caused by the channel. With this information, it is possible to describe the channel and equalize the data.

In this study, we will evaluate the performance of various channel estimation techniques. The estimators selected for comparison have been carefully chosen based on their relevance and effectiveness in the context of our investigation:

A. LS

The least squares (LS) channel estimator yields the estimation of the channel's frequency response at the pilot tone positions as referenced in [23]

$$\hat{H}(k) = \frac{\hat{s}_p(k)}{s_p(k)}, \quad (5)$$

where $\hat{s}_p(k)$ represents the received signal on the k -th subcarrier in the frequency domain, while $s_p(k)$ denotes the pilot signal transmitted on the k -th subcarrier. Following the estimation process, a linear interpolation technique is employed to derive the channel's frequency response across all subcarriers within the OFDM symbol.

B. SVR

SVR is an extension of the widely-known Support Vector Machine (SVM) technique, initially proposed by Drucker et al. [24]. While SVM aims to find an optimal hyperplane for classification tasks, SVR seeks an optimal hyperplane with an ε -tube around it to accommodate a continuous output variable. This ε -tube ensures that most data points fall within its boundaries. Like SVM, SVR employs the kernel trick to map the input data into a higher-dimensional feature space, facilitating linear regression analysis.

Considering that SVR was originally designed to operate on real-valued samples [25], we adapt our methodology to handle OFDM symbols, which are typically complex-valued. Our proposed SVR estimator is divided into two parallel estimators, each focusing on either the real part $\Re(y[n])$ or the imaginary part $\Im(y[n])$ of the OFDM symbol. For simplicity and clarity, we detail only the estimation process for the real part below, as the development for the imaginary part is analogous.

Considering the slack variables ξ_i^+ and ξ_i^- , respectively, for the positive and negative components in the real part, we arrive at a formulation whose task boils down to minimizing:

$$\frac{1}{2} \|H_p(k)\|^2 + C \sum_{i=1}^l (\xi_i^+ + \xi_i^-), \quad (6)$$

subject to

$$\Re(y[n]) - \sum_{k \in \kappa_p} \Re(s_p(k) H_p(k) e^{j2\pi \frac{k}{K} n}) \leq \varepsilon + \xi_i^+; \quad (7)$$

$$-\Re(y[n]) + \sum_{k \in \kappa_p} \Re(s_p(k) H_p(k) e^{j2\pi \frac{k}{K} n}) \leq \varepsilon + \xi_i^-; \quad (8)$$

$$\xi_i^+, \xi_i^- \geq 0, \quad (9)$$

where l is the number of training constraints (i.e., slack variable pairs) derived from the real-valued received samples.

In the imaginary part, a similar procedure is performed. The positive constant C determines the trade-off between the flatness of the hyperplane and the amount up to which deviations larger than ε are tolerated [3].

By making zero the primal-dual functional gradient with respect to $H_p(k)$, we get the Lagrange multipliers φ_n^+ and φ_n^- for the positive and negative components, respectively. The expression for channel estimated real values at pilot positions is:

$$\Re(\hat{H}_p(k)) = \sum_{n=1}^{K-1} (\varphi_n^+ - \varphi_n^-) \Re(s_p(k)), \quad (10)$$

After estimating the real and imaginary parts of $\hat{H}_p(k)$, we combine the values to obtain the complex estimation of $\hat{H}_p(k)$.

SVR allows for the use of different kernel functions such as linear, polynomial, or radial basis function (RBF). The choice of kernel depends on the nature of the problem and the characteristics of the dataset. In this study, we employ a variety of kernels, including traditional ones such as the linear and RBF, alongside the innovative quantum kernel.

C. K-Means

Traditional channel estimation methods rely on pilot signals, which consume spectral resources and reduce efficiency. An alternative approach is to use unsupervised learning techniques, such as K-Means, to estimate the channel directly from the received symbols, eliminating the need for pilots [11]. In this context, K-Means is applied to group the received symbols into clusters that correspond to the modulated constellation points.

K-Means is an unsupervised learning algorithm widely used for data clustering, which organizes unlabeled data points into distinct groups based on similarity. Unlike supervised methods, the input data used by K-Means does not have predefined class labels. Instead, the algorithm iteratively partitions the data into clusters by minimizing intra-cluster variance, making it particularly suitable for problems where underlying structure must be inferred directly from the data.

Clustering algorithms can be classified as exclusive, overlapping, hierarchical, or probabilistic. K-Means falls under the “exclusive” or “hard” clustering category, where each data point belongs strictly to one cluster. This type of analysis is commonly applied in domains such as market segmentation, document and image clustering, and compression tasks, owing to its conceptual simplicity and computational efficiency. As a centroid-based method, K-Means operates by initializing cluster centroids and refining them iteratively to minimize the distance between data points and their assigned centroid. The centroid, which represents the center of a cluster, is typically computed as the mean of all points in that cluster.

In a communication system employing QPSK modulation, the received symbols naturally form four clusters in the complex plane, each corresponding to a different symbol in the constellation [26]. Given N received symbols and $M = 4$ expected clusters, the centroid of each cluster S_m , denoted $c_{m,k}$, is calculated as the average of the symbols assigned to that cluster [27]:

$$c_{m,k} = \frac{1}{|S_m|} \sum_{\hat{s}_k \in S_m} \hat{s}_k, \quad m = 1, 2, 3, 4, \quad (11)$$

where \hat{s}_k represents the received symbol at subcarrier k .

Assuming normalized QPSK symbols (unitary magnitude: $|s_m| = 1$), the centroids $c_{m,k}$ approximate the channel response H_k scaled by the transmitted symbols s_m . The channel’s amplitude A_k and phase θ_k at subcarrier k are derived as follows:

$$A_k = \exp \left(\operatorname{Re} \left(\frac{1}{4} \sum_{m=1}^4 \log(c_{m,k}) \right) \right), \quad (12)$$

where the logarithmic averaging cancels noise and isolates the channel gain. And

$$\theta_k = \operatorname{Im} \left(\frac{1}{4} \sum_{m=1}^4 \log(c_{m,k}) - \pi \right), \quad (13)$$

where subtracting π corrects for the inherent $\frac{\pi}{4}$ -rotational symmetry of QPSK symbols. Finally, the estimated channel response at each subcarrier is given by:

$$\hat{H}(k) = A_k e^{j\theta_k}. \quad (14)$$

This method has advantages over least squares (LS)-based estimation, as the noise effect can be mitigated through the averaging operation on the clusters, making the method more robust to additive noise.

Although classical K-Means provides a viable approach to pilotless channel estimation, its computational complexity can become a limiting factor, especially for large-scale scenarios. To address this, we will later introduce a QK-Means algorithm, which aims to improve clustering efficiency and potentially improve the overall estimation performance.

IV. QUANTUM METHODS FOR CHANNEL ESTIMATION

A. Quantum Kernels

Quantum kernels play a fundamental role in QML by using quantum computing principles to process and analyze data. They extend classical kernel methods into a quantum framework, allowing the representation of complex data structures in higher-dimensional quantum feature spaces [28]–[30]. This approach is particularly advantageous in learning tasks where conventional methods struggle to efficiently capture intricate relationships, such as in high-dimensional or nonlinearly separable problems [31].

At the core of quantum kernel methods lies the quantum feature map, which implements the kernel trick in a quantum setting [29]. A quantum feature map is a function $\phi : \mathcal{X} \rightarrow \mathcal{H}$ that embeds a classical data point \mathbf{x} into a corresponding quantum state in a Hilbert space. The quantum kernel function $K(\mathbf{x}_i, \mathbf{x}_j)$ measures the similarity between two data points \mathbf{x}_i and \mathbf{x}_j by computing the fidelity between their respective quantum feature states $|\phi(\mathbf{x}_i)\rangle$ and $|\phi(\mathbf{x}_j)\rangle$. Mathematically, the quantum kernel is defined as:

$$K(\mathbf{x}_i, \mathbf{x}_j) = |\langle \phi(\mathbf{x}_i) | \phi(\mathbf{x}_j) \rangle|^2. \quad (15)$$

Here, the quantum feature states are generated by applying a parameterized unitary transformation $\mathcal{U}_{\phi(\mathbf{x})}$ to an initial reference state:

$$|\phi(\mathbf{x}_i)\rangle = \mathcal{U}_{\phi(\mathbf{x}_i)}|0\rangle. \quad (16)$$

On a quantum computer, the kernel matrix is estimated by executing a quantum circuit for each pair of training samples [32]. The kernel value, which reflects the fidelity of two quantum states, can be approximated by measuring the probability of obtaining an all-zero bit-string in the computational (Z) basis. During inference, the prediction for a new data point \mathbf{x} is performed by computing its kernel similarity with the support vectors, which typically form a small subset of the training data, thereby reducing the computational overhead compared to evaluating against all training samples [33].

B. Pauli Feature Maps

The Pauli Feature Map, introduced by Havlíček et al. [30], is a quantum feature mapping method that uses Pauli gate operations to efficiently encode classical data into quantum states. This encoding enables the representation of higher-order correlations between input data points, allowing quantum kernel methods to capture complex relationships that may not be easily discernible using classical approaches. Such

capabilities are particularly useful in tasks like classification, regression, and clustering, where accurately capturing data dependencies is crucial for predictive performance.

This mapping transforms an input vector $\mathbf{x} \in \mathbb{R}^d$ into an d -qubit quantum state $|\psi(\mathbf{x})\rangle$ by applying a unitary operator

$$\mathcal{U}_{\Phi(\mathbf{x})} = \prod_r U_{\Phi(\mathbf{x})} H^{\otimes d}, \quad (17)$$

where

$$U_{\Phi(\mathbf{x})} = \exp\left(i \sum_{S \in \mathcal{I}} \phi_S(\mathbf{x}) \prod_{k \in S} P_k\right). \quad (18)$$

In this formulation S denotes a set of qubit indices describing the connectivity of the feature map, \mathcal{I} is the collection of all such index sets and $P_k \in \{\mathbb{I}, X, Y, Z\}$ are Pauli operators applied in the encoding. The operator H represents the Hadamard gate, which is applied to each qubit in the initial state as $H^{\otimes d}$. The variable r is the number of repetitions in (17) to obtain $\mathcal{U}_{\Phi(\mathbf{x})}$. The encoding function is defined as follow:

$$\phi_S : \mathbf{x} \mapsto \begin{cases} x_i & \text{if } S = \{i\}, \\ (\pi - x_i)(\pi - x_j) & \text{if } S = \{i, j\}. \end{cases} \quad (19)$$

The encoding function (19) was designed to capture both individual feature contributions (x_i) and pairwise interactions (x_i, x_j), enabling the quantum model to represent complex data relationships in the Hilbert space [30]. However, other encoding strategies may be considered depending on the problem at hand. Recent works have explored methods to analyze and optimize quantum feature maps, including criteria for determining their suitability for classification tasks [34].

C. QSVR

In our study, we integrate a 5-qubit quantum kernel into SVR algorithm for channel estimation in OFDM systems. The QSVR model takes advantage of quantum-enhanced feature mapping to improve estimation accuracy, capturing complex non-linear relationships within the received signal. The number of pilot tones, crucial for an accurate estimation, corresponds to the number of qubits in our quantum model.

To configure the QSVR model effectively, we systematically explored different hyperparameters, including: (i) feature encoding functions, (ii) Pauli matrix sequences, (iii) number of repetitions, and (iv) types of entanglement, evaluating their impact on performance. These configurations were implemented using the PauliFeatureMap class from the Qiskit Python package [35]. Specifically, the number of repetitions (r) refers to how many times the encoding function is applied, influencing the richness of the feature space, while the type of entanglement determines how qubits are interconnected, affecting how information is distributed across the quantum system.

For illustration, consider a 2-qubit feature map with the following configuration: (1) Encoding function $\phi_S(\mathbf{x}) = \phi_S$; (2) Interaction set $\mathcal{I} = \{\{1\}, \{2\}, \{1, 2\}\}$; (3) Pauli operators P_k , where each P_k is a Pauli Z matrix acting on the k -th qubit. With this setup, Equation (18) simplifies to:

$$U_{\phi(\mathbf{x})} = e^{(i(x_1 Z_1 + x_2 Z_2 + (\pi - x_1)(\pi - x_2) Z_1 Z_2))}. \quad (20)$$

The sequence of Pauli matrices Z_1, Z_2 , and $Z_1 Z_2$ in Eq. (20) is represented as $[Z, Z, ZZ]$, which corresponds to the ZZFeatureMap. This example clarifies the notation used to define Pauli sequences in our feature maps [30].

During our experimental setup, we tested multiple feature encoding functions, specifically those proposed by Suzuki et al. [34], as well as different Pauli matrix sequences of the form:

$$[P_1, P_2, P_3 P_4], \quad \text{with } P_i \in \{\mathbb{I}, X, Y, Z\}. \quad (21)$$

Additionally, we explored various entanglement structures, ranging from linear to full connectivity, and examined different values for the number of repetitions in the encoding layers. After extensive testing across these configurations, we found that the best results were achieved using the ZZFeatureMap as the feature map, linear connectivity for entanglement, and a single repetition ($r = 1$).

Although this configuration yielded the most accurate results, the underlying reasons for its superiority are not yet fully understood. Further exploration into how entanglement topology and encoding depth influence model performance may provide deeper insights into this behavior. In particular, the role of entanglement in enhancing the learning capacity of quantum kernels remains an open question.

While numerous configurations were tested, we present results for the best-performing case, as it provides the most relevant insights into the potential of QSVR for channel estimation. A more detailed investigation of the impact of different encoding choices is beyond the scope of this work but remains an important direction for further understanding the effectiveness of quantum kernels in communication systems.

D. QK-Means

The distance calculation in the K-Means algorithm can be improved using a quantum approach to estimate the distances between dataset points more efficiently [36]. In this section, we describe how distance computation is performed in the quantum version of K-Means.

First, we encode two classical data points, \mathbf{x} and \mathbf{y} , which are complex numbers, into the quantum states $|x\rangle$ and $|y\rangle$, respectively. This is achieved by applying the U_3 gate to the initial state $|0\rangle$, preparing the desired quantum states. The U_3 gate is defined as

$$U_3(\theta, \pi, 0) = \begin{bmatrix} \cos\left(\frac{\theta}{2}\right) & -e^{i\pi} \sin\left(\frac{\theta}{2}\right) \\ e^{i\pi} \sin\left(\frac{\theta}{2}\right) & \cos\left(\frac{\theta}{2}\right) \end{bmatrix}, \quad (22)$$

where θ represents the phase of the complex number being encoded.

Once the data points are encoded, we apply the SWAP test to compute the distance between them based on the orthogonality of their quantum states. Let $|x\rangle$ and $|y\rangle$ be the quantum states obtained after applying the Hadamard gate and angle encoding to the initial $|0\rangle$ states.

To implement the SWAP test, we first create a superposition by applying a Hadamard gate to an ancilla qubit, $|0_{\text{anc}}\rangle$. We then perform a controlled-SWAP operation, using $|0_{\text{anc}}\rangle$ as the

control qubit. Finally, another Hadamard gate is applied to the ancilla, leading to the transformation:

$$|0_{\text{anc}}\rangle |x\rangle |y\rangle \rightarrow \begin{cases} \frac{1}{2} |0_{\text{anc}}\rangle (|x\rangle |y\rangle + |y\rangle |x\rangle) + \\ \frac{1}{2} |1_{\text{anc}}\rangle (|x\rangle |y\rangle - |y\rangle |x\rangle). \end{cases} \quad (23)$$

The complete quantum circuit is illustrated in Fig. 2:

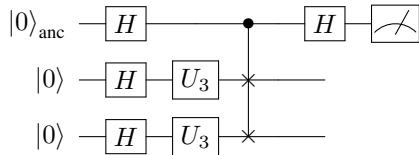


Fig. 2: Swap Test circuit used to estimate the inner product between two quantum states.

The probability of measuring $|0_{\text{anc}}\rangle$ is given by:

$$P(0_{\text{anc}}) = \frac{1}{2} + \frac{1}{2} |\langle x|y\rangle|^2. \quad (24)$$

The term $|\langle x|y\rangle|^2$ quantifies the similarity between quantum states $|x\rangle$ and $|y\rangle$, enabling distance inference between data points \mathbf{x} and \mathbf{y} . The fidelity measure, computed via the SWAP test circuit, serves as the basis for minimizing the clustering objective function:

$$\arg \min_{\mathbf{S}} \sum_{i=1}^k \sum_{\mathbf{x} \in S_i} (1 - |\langle \mathbf{x} | c_i \rangle|^2), \quad (25)$$

where c_i represents the centroid of cluster S_i . The algorithm proceeds through classical K-Means iterations (Section III-C), with quantum distances maintaining accuracy as shown in Figs. 3, 4, and 5, consistent with prior work [36], [37].

E. Complexity of Classical and Quantum Models

Channel estimation in CP-free OFDM presents significant computational challenges, including increased computational load due to larger search spaces in estimation algorithms and instability in traditional methods when dealing with impulsive noise and high-dimensional frequency-selective channels. These challenges are particularly pronounced in frequency-selective channels affected by impulsive noise. Classical methods, such as LS and MMSE estimators, face trade-offs between computational efficiency and accuracy, particularly in CP-free OFDM where inter-symbol interference and noise sensitivity are exacerbated. Although MMSE provides better performance in frequency selective channels, its computational cost makes it prohibitive for practical applications. To address these limitations, this study investigates the potential of QSVR and QK-Means for CP-free OFDM channel estimation. Using quantum kernel methods and quantum clustering techniques, these approaches aim to improve feature representation and computational scalability, particularly in frequency-selective and impulsive noise environments.

Classical SVR is a well-established regression technique for channel estimation [38], [39]; however, its worst-case

computational complexity of $O(N^3)$ in the quadratic programming step can be a major limitation, particularly in real-time OFDM systems with high subcarrier counts and rapidly changing channel conditions. In practice, heuristic methods such as SMO [40] and sparse approximations [41] can significantly reduce the effective complexity, making SVR feasible in some real-time scenarios, though these techniques often involve trade-offs in accuracy and adaptability. In scenarios where the channel impulse response (CIR) is highly frequency selective, the dimensionality of the channel estimation problem in OFDM systems can increase significantly, exacerbating the computational burden. These challenges motivate the exploration of alternative approaches, such as quantum-enhanced regression techniques, to achieve more scalable and efficient channel estimation.

The computational complexity of classical and quantum methods diverges significantly in high-dimensional regimes, as summarized in Table I, where N represents the number of training samples and d is the data dimension. Classical methods often struggle with the exponential growth of feature space dimensionality, leading to increased computational burden and inefficient scalability. In contrast, quantum methods, particularly those utilizing Quantum Random Access Memory (QRAM), can efficiently encode and access high-dimensional data representations, enabling computational advantages over classical approaches [42]. As shown in Table I, QRAM-based quantum algorithms demonstrate improved scaling in kernel-based learning tasks.

Criterion	Classical SVR	QSVR [42]
Kernel Evaluation	$O(d)$	$O(\log N)$
Kernel Matrix	$O(N^2 d)$	$O(\log N d)$
Training	$O(N^3)$	$O(\log N d)$
Data Dimensionality	Struggles for $d \sim 10^3$	Handles exponential d

TABLE I: Comparison of computational complexity for SVR and QSVR approaches.

QSVR takes advantage of quantum kernel methods to encode frequency-domain channel data into high-dimensional Hilbert spaces. As discussed in [30], quantum kernels enable implicit feature mapping, which in certain cases may lead to improved model expressiveness. However, practical computational speedups remain contingent on efficient quantum data access and noise robustness, as current quantum kernel evaluations scale at least quadratically in N and require $O(N^3)$ measurements to maintain generalization performance in the presence of noise [43]. Our experimental results on quantum simulators suggest that QSVR can enhance regression performance in 16-QAM modulation scenarios, particularly in the presence of sparse, high-magnitude noise. This improvement appears to stem from the expressive power of quantum feature maps in capturing nonlinear channel distortions and reducing prediction error. However, further investigation is required to validate these advantages on real quantum hardware.

The computational advantages of quantum methods extend beyond regression tasks to unsupervised learning paradigms such as clustering. Classical K-Means, a cornerstone algorithm for partitioning data into M groups [44], faces scalability

bottlenecks in CP-free OFDM systems when clustering data in the presence of ISI or with impulsive noise. Each iteration of classical K-Means involves calculating pairwise Euclidean distances between N data points and M centroids in d -dimensional space ($O(NMd)$), assigning points to the nearest cluster ($O(NM)$), and updating centroids ($O(Nd)$), resulting in an overall per-iteration complexity of $O(NMd)$. While heuristic optimizations exist, the quadratic dependence on N , M , and d becomes prohibitive for real-time applications with dynamic channel conditions.

QK-Means addresses these limitations by redesigning key steps through quantum parallelism [42]. Data points are encoded into $O(\log N)$ qubits via amplitude embedding [45], a process requiring $O(N \log N)$ initial operations to prepare quantum states. Once encoded, quantum subroutines replace classical computations: distances are calculated using Swap tests [46] with $O(\log N)$ complexity per data-centroid pair (assuming parallel execution across all pairs), and Grover’s search [47] reduces cluster assignment from $O(M)$ to $O(\sqrt{M})$ per point. However, centroid updates remain classical ($O(Nd)$) because computing the mean of quantum-encoded data requires measurement, which collapses quantum superposition into classical values.

A detailed comparison of classical and quantum K-Means complexities is provided in Table II. While the quantum variant theoretically reduces scaling in distance and assignment steps, its practical efficacy depends on efficient state preparation and error-resilient hardware. For example, the $O(N \log N)$ initialization cost of amplitude embedding, often underemphasized in theoretical analyses, can dominate the run time for small N . Additionally, Swap tests require high-fidelity qubits to preserve coherence in parallel execution, making large-scale implementations challenging. These constraints are similar to those in QSVM, where quantum kernel evaluations depend on stable quantum hardware and, in some cases, efficient QRAM access.

Step	K-Means	QK-Means
Initial Encoding	$O(1)$	$O(N \log N)$
Distance Calculation	$O(NMd)$	$O(NM \log N)$
Cluster Assignment	$O(NM)$	$O(N\sqrt{M})$
Centroid Update	$O(Nd)$	$O(Nd)$

TABLE II: Computational complexity comparison between K-Means and QK-Means.

V. RESULTS

To validate the proposed QSVM and the QK-Means approach, and to compare their performance against the classical SVR and LS in channel estimation, we analyzed mean square error (MSE) curves, where

$$MSE = E[|H - \hat{H}|^2] \quad (26)$$

considering the simulation parameters summarized in Table III.

In the proposed QSVM estimator, each pilot tone used during channel estimation gives rise to one feature in the

Parameter	Value
Number of subcarriers (K)	16
Subcarrier modulation	QPSK and 16-QAM
Cyclic prefix length (subcarriers)	4 and 0
Number of pilot subcarriers (S_p)	5
channel impulse response	[1 0 0.3 + j 0.3]
channel coherence band (in terms of system bandwidth)	0.5

TABLE III: Simulation parameters.

regression model, and the Pauli-based quantum feature map encodes these features using one qubit per dimension. Consequently, the number of qubits is exactly equal to the number of pilot tones. In standard OFDM configurations, increasing the number of subcarriers typically requires increasing the number of pilot tones to maintain estimation accuracy and avoid excessive interpolation gaps. Under this feature-map architecture, such an increase will proportionally increase the number of qubits and thus the size of the quantum circuit. Because the cost of simulating quantum circuits grows exponentially with the number of qubits, large OFDM scenarios are not computationally feasible on classical hardware. For this reason, our study focuses on a controlled comparative analysis under a tractable configuration rather than on scalability optimization. Future work may explore adaptive pilot strategies or alternative quantum encodings that reduce qubit requirements.

Since our goal is to evaluate the performance of the algorithms in a frequency-selective wireless channel, we selected a two-tap multipath channel with impulse response given by $h[n] = \delta[n] + (0.3 + 0.3j)\delta[n - 2]$, i.e., $h = [1 \ 0 \ 0.3 + 0.3j]$, [48]. This channel model meets the requirements for the proposed tests.

In this work, the unit was considered in terms of subcarriers (since the channel is discrete and normalized by the sampling rate), so we can consider that the coherence bandwidth of the channel is: $B_c \approx \frac{1}{T_{max}} = \frac{1}{2} = 0.5$ (in terms of normalized frequency or system bandwidth).

To enable testing with all estimators, a packet-based transmission was considered. For the SVR and QSVM estimators, each packet consists of a header formed by two OFDM symbols containing only the pilot tones in their specific positions $s_p(k)$, $k \in \kappa_p$ and zero in the other subcarriers. These two symbols will generate two sequences of 16 samples in the time domain, which will be used to obtain the support vectors of the regressor, as described in section III-B. For the LS estimator, each packet contains 10 OFDM symbols containing data and interleaved pilots, in the proportion 3 : 1. At the pilot positions, the frequency response of the channel is estimated, and then a linear interpolation is performed. And, in the K-Means and QK-Means estimators, packets with 10 OFDM symbols containing only data were used to obtain the centroid and estimate the channel, as described in section III-C. For each estimator, 100 packets were transmitted to calculate the average and estimate the MSE .

We studied the performance variation in the system due to changes in the kernel and free parameters of the SVR, the type of coding of the classical data into quantum ones in the

QSVR and the amount of data required for the estimation using K-Means and QK-Means. For the SVM-based estimators, we tested the linear, radial and polynomial kernels and varied the parameter C from 1 to 1000. The optimal parameter found for C was $C = 100$, and kernel RBF. To generate the quantum kernel and calculate the distance between the centroids and samples in the QK-Means, we used the Qiskit Python package [49] to execute the tasks in a local quantum simulator. The number of blocks transmitted in the K-Means and QK-Means estimator was gradually increased until perfect convergence in the average was observed, this fact was obtained with the transmission of around 1000 blocks. Fig. 3 shows the MSE performance as a function of the signal-to-noise ratio (SNR) for the first test with cyclic prefix and Gaussian noise.

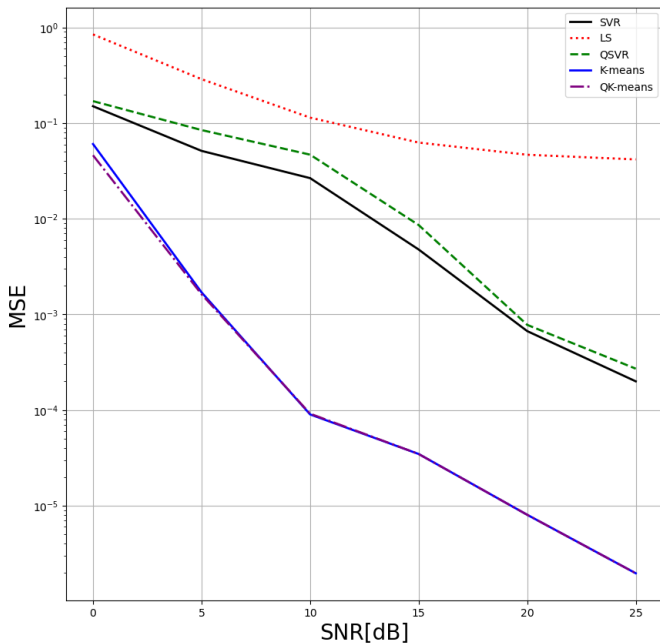


Fig. 3: MSE performance comparison in OFDM system with CP and AWGN.

Analyzing the performance of the MSE obtained from the tested estimators, we observe in Fig. 3 that the MSE curve obtained with the LS estimator does not decay due to the small number of pilot tones, which caused significant spacing between them and poor estimation of the interpolated subcarriers. Several tests, varying the number of subcarriers and pilot tones, were performed with the LS estimator and corroborate the conclusion presented. In contrast, the curves obtained with the SVR, QSVR, K-Means and QK-Means estimators demonstrate good performance in terms of MSE. It is important to remember that K-Means and QK-Means, because they do not use pilot tones, act on all subcarriers and, therefore, do not require interpolation, in addition to requiring a large volume of data for perfect convergence to the mean, demanding a large volume of data processing and increasing the computational complexity of the system. Another point that deserves attention is that the interpolation of SVR and QSVR is performed during the FFT, since the estimation is

performed in the time domain. This fact reduces the volume of data processing and the computational complexity of the system.

Fig. 4 shows the MSE performance as a function of SNR for the second test, where the system operates with a CP and is subject to impulsive noise. The impulse noise distortion follows a Bernoulli–Gaussian process with $p = 0.05$ and the impulse power is set 20 dB higher than the signal variance at the receiver input. The MSE curves for the LS and SVR estimators remain unchanged compared to the first test, which was performed without impulsive noise. This suggests that, under the adopted transmission parameters, impulsive noise has a negligible impact on these estimators. In contrast, the MSE curves obtained with the QSVR, K-Means and QK-Means estimators show a worsening in performance, likely due to their sensitivity to impulsive noise. However, QSVR maintains the expected reduction in MSE as SNR increases, suggesting that the quantum kernel retains useful structural properties from the input data despite this degradation. This behavior can be attributed to the quantum kernel’s ability to map input data into a higher-dimensional Hilbert space, making samples more distinguishable. As SNR increases, the impact of noise diminishes, allowing the quantum feature map to better preserve the underlying data structure. Consequently, the model’s generalization capability improves, leading to a steady decline in error. The expressibility of the quantum feature map plays a key role in this process, as an effective mapping enhances the robustness of the regression model, ensuring error reduction even in the presence of some performance degradation.

These results indicate that impulsive noise slightly changes the input signal characteristics, which are analyzed in more detail below. Additionally, a plateau is observed in the MSE curves of the K-Means and QK-Means estimators, suggesting their increased susceptibility to impulsive noise. This behavior implies that their clustering-based structure struggles to adapt effectively to the presence of non-Gaussian noise.

In the third test, the CP was removed from the system while the impulsive noise and AWGN were maintained. The MSE performance as a function of SNR for this test is shown in Fig. 5, where we observe that the MSE curves for LS, SVR and QSVR estimators remain nearly unchanged compared to previous tests with CP. This result suggests that the absence of CP does not significantly affect the performance of these estimators under the adopted transmission parameters. Conversely, the MSE curves for K-Means and QK-Means show a significant deterioration, reinforcing their sensitivity to interference noise, likely due to the clustering-based structure, which may struggle with the increased symbol dispersion in the absence of CP.

To further investigate the slightly worse performance of QSVR compared to SVR, a final test was conducted using a different modulation scheme. This test was motivated by the use of QPSK modulation, where symbol differences are only in phase, while amplitude remains constant. We assumed that this behavior could be more appropriate to the RBF kernel used in SVR than to the quantum kernel of QSVR, which may depend on broader feature distributions. To evaluate this, we

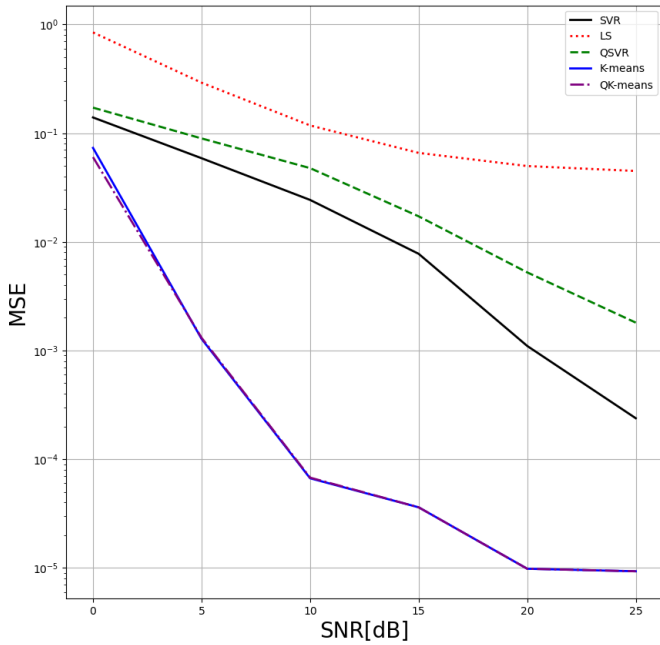


Fig. 4: MSE performance comparison in OFDM system with CP and impulsive noise

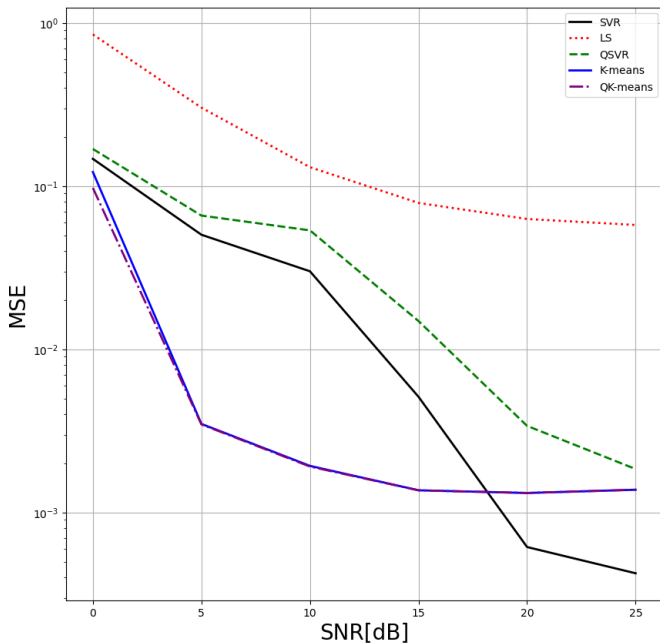


Fig. 5: MSE performance comparison in OFDM system with impulsive noise and without CP.

tested the 16-QAM modulation, which introduces both phase and amplitude variations in the constellation. In this test we included the LMMSE algorithm with the channel correlation matrix and Gaussian noise variance known to the receiver [50]. The purpose of this inclusion is to observe the behavior of a classical optimal algorithm with the parameters adopted in this simulations. The results, presented in Fig. 6 confirm that QSVR outperforms SVR in this setting, supporting the idea that the performance of QSVR is strongly influenced by the

nature of the training samples and how they are mapped into quantum bits during kernel generation. The K-Means and QK-Means estimators were not included in this test, since they were developed for QPSK modulations and their study for 16-QAM modulation is beyond the scope of this work. Since, with 16 centroids of different amplitudes and phases, obtaining the unambiguous channel frequency response becomes a new problem to be investigated. The LS estimator performed very poorly, as expected, due to its inability to efficiently deal with interfering noise, as discussed in previous tests. The LMMSE estimator performed very similarly to the LS estimator, and this is justified by the same reasons. Tests were also performed with the LMMSE in various scenarios, which corroborated the conclusion reached, showing that improving its performance requires a larger number of pilots.

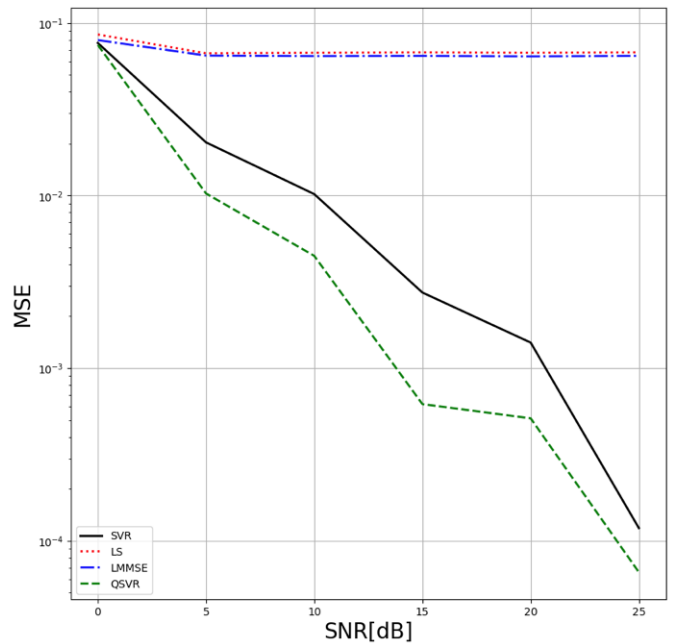


Fig. 6: MSE performance comparison in OFDM system with-out CP with 16-QAM modulation.

VI. CONCLUSIONS

This work investigated the application of QML techniques, specifically QSVR and QK-Means, for channel estimation in OFDM systems. While these algorithms are established in the ML literature, their use in wireless communications is still limited. By adapting them to OFDM channel estimation and evaluating their performance under various transmission conditions, this study contributes to bridging QML and communication systems. Simulations covered realistic scenarios including AWGN, impulsive noise, limited pilot density, and absence of CP. The LS and LMMSE estimator showed poor performance in pilot-sparse environments due to interpolation and noise sensitivity. K-Means and QK-Means performed well under AWGN without requiring pilots but demanded large datasets and were vulnerable to impulsive noise and ISI. Both SVR and QSVR demonstrated robustness under such adverse conditions, with QSVR outperforming SVR in multilevel

modulations like 16-QAM, indicating the quantum kernel's superior ability to extract structural features from input data. Although the experiments relied on classical simulations, the results suggest that using scalable quantum hardware with idealized QRAM could significantly reduce computational complexity. This study reinforces the feasibility and potential benefits of applying QML to wireless communication tasks.

Future work may explore more advanced quantum kernel architectures tailored for communication signals, integration with quantum channel models, and the application of these methods in emerging areas such as 6G networks and massive MIMO. Additionally, Blind channel estimation study with K-Means and 16-QAM modulation. And, investigating hybrid quantum-classical schemes that combine quantum feature extraction with classical post-processing may offer a promising path toward practical deployment in near-term quantum devices.

REFERENCES

- [1] V. Tarokh *et al.*, *New directions in wireless communications research*. New York: Springer, 2009.
- [2] A. F. Molisch, *Orthogonal Frequency Division Multiplexing (OFDM)*. New York: IEEE, 2011, pp. 417–443, doi: 10.1002/9781119992806.ch19.
- [3] N. S. Beena Ballal, Ankit Chadha, “Orthogonal frequency division multiplexing and its applications,” *International Journal of Science and Research*, vol. 2, no. 1, pp. 325–328, 2013, doi = 10.48550/arXiv.1309.7334.
- [4] B. Wang and K. R. Liu, “Advances in cognitive radio networks: A survey,” *IEEE Journal of Selected Topics in Signal Processing*, vol. 5, no. 1, pp. 5–23, 2011, doi = 10.1109/JSTSP.2010.2093210.
- [5] Z. Du, X. Song, J. Cheng, and N. C. Beaulieu, “A channel estimation technique for ofdm systems in dispersive time-varying channels,” in *2009 11th Canadian Workshop on Information Theory*, 2009, pp. 173–176, doi = 10.1109/CWIT.2009.5069548.
- [6] D. Shrestha, X. Mestre, and M. Payaró, “On channel estimation for power line communication systems in the presence of impulsive noise,” *Computers & Electrical Engineering*, vol. 72, pp. 406–419, 2018, doi = 10.1016/J.COMPELECENG.2018.10.006.
- [7] M. Sanchez-Fernandez, M. de Prado-Cumplido, J. Arenas-Garcia, and F. Perez-Cruz, “Svm multiregression for nonlinear channel estimation in multiple-input multiple-output systems,” *IEEE Transactions on Signal Processing*, vol. 52, no. 8, pp. 2298–2307, 2004, doi = 10.1109/TSP.2004.831028.
- [8] D. Sebal and J. Bucklew, “Support vector machine techniques for nonlinear equalization,” *IEEE Transactions on Signal Processing*, vol. 48, no. 11, pp. 3217–3226, 2000, doi = 10.1109/78.875477.
- [9] L. V. Nguyen, A. L. Swindlehurst, and D. H. N. Nguyen, “Svm-based channel estimation and data detection for one-bit massive mimo systems,” *IEEE Transactions on Signal Processing*, vol. 69, pp. 2086–2099, 2021, doi = 10.1109/TSP.2021.3068629.
- [10] O. Simeone, “A very brief introduction to machine learning with applications to communication systems,” *IEEE Transactions on Cognitive Communications and Networking*, vol. 4, no. 4, pp. 648–664, 2018, doi = 10.1109/TCCN.2018.2881442.
- [11] K. Jung and H. Wang, “Pilotless channel estimation scheme using clustering-based unsupervised learning,” in *2018 15th International Symposium on Wireless Communication Systems (ISWCS)*, 2018, pp. 1–5, doi = 10.1109/ISWCS.2018.8491198.
- [12] S. Cherkaoui, “*Quantum Leap: Exploring the Potential of Quantum Machine Learning for Communication Networks*,” in *Proceedings of the Int'l ACM Conference on Modeling Analysis and Simulation of Wireless and Mobile Systems*, ser. MSWiM '23. New York, NY, USA: Association for Computing Machinery, 2023, pp. 5, doi = 10.1145/3616388.3625543.
- [13] M. Mafu, “Advances in artificial intelligence and machine learning for quantum communication applications,” *IET Quantum Communication*, vol. 5, no. 3, pp. 202–231, 2024, doi = 10.1049/qt2.12094.
- [14] B. Narottama, Z. Mohamed, and S. Aïssa, “Quantum machine learning for next-g wireless communications: Fundamentals and the path ahead,” *IEEE Open Journal of the Communications Society*, vol. 4, pp. 2204–2224, 2023, doi = 10.1109/OJCOMS.2023.3309268.
- [15] N. Ishikawa, G. T. F. de Abreu, P. Popovski, and R. W. Heath, “Quantum-accelerated wireless communications: Concepts, connections, and implications,” *arXiv preprint arXiv:2506.20863*, 2025, doi = 10.48550/arXiv.2506.20863.
- [16] V. B. Chalampalem, S. Nagaraju, R. K. Kumar, and T. Santhivandana, “Quantum machine learning enhanced sdr architecture for adaptive and secure wireless communication using oqam,” *Research Square Preprint*, 2025, doi = 10.21203/rs.3.rs-7239745/v1.
- [17] K. Hwang, H.-T. Lim, Y.-S. Kim, D. K. Park, and Y. Kim, “Distributed quantum machine learning via classical communication,” *Quantum Science and Technology*, vol. 10, no. 1, p. 015059, Dec. 2024, DOI=10.1088/2058-9565/ad9cb9.
- [18] D. Bhoumik, S. Sur-Kolay, L. K. K. J., and S. S. Iyengar, “Synergy of machine learning with quantum computing and communication,” 2023. [Online]. Available: <https://arxiv.org/abs/2310.03434>
- [19] T. B. D. Authors, “Quantum fisher-preconditioned reinforcement learning: From single-qubit control to rayleigh-fading link adaptation,” *Journal Name TBD*, 2025.
- [20] ———, “Quantum machine learning enhanced sdr architecture for adaptive and secure wireless communication using oqam,” *Journal Name TBD*, 2025.
- [21] M. Ghosh, “Analysis of the effect of impulse noise on multicarrier and single carrier qam systems,” *IEEE Transactions on Communications*, vol. 44, no. 2, pp. 145–147, 1996, doi: 10.1109/26.486604.
- [22] M. Fernandez-Getino Garcia, J. Paez-Borralló, and S. Zazo, “Dft-based channel estimation in 2d-pilot-symbol-aided ofdm wireless systems,” in *IEEE VTS 53rd Vehicular Technology Conference*, Spring 2001. Proceedings (Cat. No.01CH37202), vol. 2, 2001, pp. 810–814, doi = 10.1109/VETECS.2001.944491.
- [23] A. Papoulis and S. Pillai, *Probability, Random Variables, and Stochastic Processes*, ser. McGraw-Hill series in electrical and computer engineering. New York: McGraw-Hill, 2002.
- [24] H. Drucker, C. J. Burges, L. Kaufman, A. Smola, and V. Vapnik, “Support vector regression machines,” *Advances in neural information processing systems*, vol. 9, 1996.
- [25] A. J. Smola and B. Schölkopf, “A tutorial on support vector regression,” *Statistics and computing*, vol. 14, pp. 199–222, 2004, doi = 10.1023/B:STCO.0000035301.49549.88.
- [26] A. Coates and A. Y. Ng, *Learning Feature Representations with K-Means*. Berlin, Heidelberg: Springer Berlin Heidelberg, 2012, pp. 561–580, doi = 10.1007/978-3-642-35289-8_30.
- [27] M. Xiao and H. Wang, “*Bit Error Rate Performance Evaluation of QPSK Signal Detected by Clustering in Deep Learning*,” 2017, doi=10.14801/JKIT.2017.15.12.117.
- [28] M. Schuld and N. Killoran, “Quantum machine learning in feature hilbert spaces,” *Phys. Rev. Lett.*, vol. 122, p. 040504, Feb 2019, doi = 10.1103/PhysRevLett.122.040504.
- [29] M. Schuld, “Supervised quantum machine learning models are kernel methods (2021),” *arXiv preprint arXiv:2101.11020*, 2023.
- [30] V. Havlíček, A. D. Córcoles, K. Temme, A. W. Harrow, A. Kandala, J. M. Chow, and J. M. Gambetta, “Supervised learning with quantum-enhanced feature spaces,” *Nature*, vol. 567, no. 7747, pp. 209–212, 2019, doi = 10.1038/s41586-019-0980-2.
- [31] Y. Liu, S. Arunachalam, and K. Temme, “A rigorous and robust quantum speed-up in supervised machine learning,” *Nature Physics*, vol. 17, pp. 1013–1017, 2021, doi = 10.1038/s41567-021-01287-z.
- [32] M. Schuld, R. Sweke, and J. J. Meyer, “Effect of data encoding on the expressive power of variational quantum-machine-learning models,” *Phys. Rev. A*, vol. 103, p. 032430, Mar 2021, doi = 10.1103/PhysRevA.103.032430.
- [33] D. K. Park, C. Blank, and F. Petruccione, “The theory of the quantum kernel-based binary classifier,” *Physics Letters A*, vol. 384, p. 126422, 2020, doi = 10.1016/j.physleta.2020.126422.
- [34] Y. Suzuki, H. Yano, Q. Gao, S. Uno, T. Tanaka, M. Akiyama, and N. Yamamoto, “Analysis and synthesis of feature map for kernel-based quantum classifier,” *Quantum Machine Intelligence*, vol. 2, p. 9, 2020, doi = 10.1007/s42484-020-00020-y.
- [35] G. A. et al, “Qiskit: An Open-source Framework for Quantum Computing,” feb 2019. [Online]. Available: <https://doi.org/10.5281/zenodo.2562111>
- [36] H. Urgelles, P. Picazo-Martínez, and J. F. Monserrat, “*Application of quantum computing to accurate positioning in 6g indoor scenarios*,” in

ICC 2022-IEEE International Conference on Communications. IEEE, 2022, pp. 643–647, doi: 10.1109/ICC45.855.2022.9838523.

- [37] S. DiAdamo, C. O’Meara, G. Cortiana, and J. Bernabé-Moreno, “Practical quantum k-means clustering: Performance analysis and applications in energy grid classification,” *IEEE Transactions on Quantum Engineering*, vol. 3, pp. 1–16, 2022, doi: 10.1109/TQE.2022.3185505.
- [38] M.-G. Garcia, J. Rojo-Alvarez, F. Alonso-Atienza, and M. Martinez-Ramon, “Support vector machines for robust channel estimation in ofdm,” *IEEE Signal Processing Letters*, vol. 13, no. 7, pp. 397–400, 2006, doi=10.1109/LSP.2006.871862.
- [39] T. Hastie, R. Tibshirani, and J. Friedman, *The Elements of Statistical Learning: Data Mining, Inference, and Prediction*, 2nd ed., ser. Springer Series in Statistics. New York: Springer, 2009, doi = 10.1007/978-0-387-84858-7.
- [40] J. Platt, “Sequential minimal optimization : A fast algorithm for training support vector machines,” Microsoft Research Technical Report, 1998.
- [41] F. Girosi, “An equivalence between sparse approximation and support vector machines,” *Neural Computation*, vol. 10, no. 6, pp. 1455–1480, 1998, doi = 10.1162/089976698300017269.
- [42] P. Rebentrost, M. Mohseni, and S. Lloyd, “Quantum support vector machine for big data classification,” *Phys. Rev. Lett.*, vol. 113, p. 130503, Sep 2014, doi = 10.1103/PhysRevLett.113.130503.
- [43] X. Wang, Y. Du, Y. Luo, and D. Tao, “Towards understanding the power of quantum kernels in the NISQ era,” *Quantum*, vol. 5, p. 531, Aug. 2021, doi = 10.22331/q-2021-08-30-531. [Online]. Available: <https://doi.org/10.22331/q-2021-08-30-531>
- [44] S. Lloyd, “Least squares quantization in pcm,” *IEEE Transactions on Information Theory*, vol. 28, no. 2, pp. 129–137, 1982, doi=10.1109/TIT.1982.1056489.
- [45] M. Schuld and F. Petruccione, *Supervised learning with quantum computers*. Switzerland: Springer, 2018, vol. 17.
- [46] S. Lloyd, M. Mohseni, and P. Rebentrost, “Quantum algorithms for supervised and unsupervised machine learning,” arXiv preprint arXiv:1307.0411, 2013, doi = 10.48550/arXiv.1307.0411.
- [47] L. K. Grover, “A fast quantum mechanical algorithm for database search,” in *Proceedings of the 29th Annual ACM Symposium on Theory of Computing*, 1996, pp. 212–219, doi = 10.48550/arXiv.quant-ph/9605043.
- [48] M. Matthe, “Basic ofdm example in python,” 2023, accessed on February 24, 2025. [Online]. Available: <https://dpsillustrations.com/pages/posts/misc/python-ofdm-example.html>
- [49] A. Javadi-Abhari, M. Treinish, K. Krsulich, C. J. Wood, J. Lishman, J. Gacon, S. Martiel, P. D. Nation, L. S. Bishop, A. W. Cross, B. R. Johnson, and J. M. Gambetta, “Quantum computing with qiskit,” 2024. [Online]. Available: <https://arxiv.org/abs/2405.08810>
- [50] O. Edfors, M. Sandell, J.-J. van de Beek, S. Wilson, and P. Borjesson, “Ofdm channel estimation by singular value decomposition,” *IEEE Transactions on Communications*, vol. 46, no. 7, pp. 931–939, 1998.



Caio Neves Silva is an undergraduate student in Computer Engineering at the Federal Center for Technological Education Celso Suckow da Fonseca (CEFET/RJ), Petrópolis, Brazil. He is a Scientific Initiation (IC) student in the Quantum Communications research group, where he works on quantum machine learning algorithms for telecommunications, including QK-Means for channel estimation and the prototyping of

a QSVR-based channel estimation approach for OFDM systems using SDR and GNU Radio. His research interests include quantum machine learning, quantum memory, and genetic algorithms.



Andrias Magno Miranda Cordeiro is an undergraduate student in Computer Engineering at the Federal Center for Technological Education Celso Suckow da Fonseca (CEFET/RJ), Petrópolis, Brazil, since 2020. He is currently a Scientific Initiation (IC) scholarship holder (2024–2025), working on quantum machine learning algorithms for communication systems.

His research interests include quantum communications, variational quantum algorithms, and circuit optimization using ZX-calculus. He has presented his work at national events, including CNMAC (“Optimizing Quantum Support Vector Machines using ZX-Calculus”) and WECIQ 2024 (“Feature Map Selection for Quantum Classifiers using Pauli Decomposition”).



João Terêncio Dias received the B.Sc. degree in Telecommunications Engineering from Fluminense Federal University (UFF), Brazil, in 2002, the M.Sc. degree in Electrical Engineering from the Military Engineering Institute (IME), Brazil, in 2006, and the Ph.D. degree in Electrical Engineering from the Federal University of Rio de Janeiro (UFRJ), Brazil, in 2013. He completed a

postdoctoral fellowship in Digital Signal Processing applied to Communication Systems at PUC-Rio in 2016. He is currently a Full Professor with the Federal Center for Technological Education of Rio de Janeiro (CEFET/RJ), Brazil, where he conducts research and supervises graduate students in telecommunications and signal processing. His research focuses on wireless communication systems, digital signal processing, communication theory, low-resolution data converters, and quantum algorithms applied to communication systems. Dr. Dias is the leader of the Quantum Communication Research Group (CQRG). He is a member of the Brazilian Telecommunications Society (SBTrT) and the IEEE.



Demerson Nunes Gonçalves is a Professor in the Department of Mathematics at CEFET/RJ, Petrópolis campus, Brazil. He received the B.Sc. degree in Mathematics Education from the Federal University of Espírito Santo in 2002 and the M.Sc. (2005) and Ph.D. (2009) degrees in Computational Modeling from the National Laboratory for Scientific Computing (LNCC), Brazil. His research lies at the intersection of

quantum physics, quantum computing, and applied mathematics. He develops quantum algorithms grounded in group-theoretic and algebraic structures, with applications to quantum machine learning, quantum cryptography, and quantum error correction. He also investigates structure-aware inference and estimation methods for communication and signal processing systems, emphasizing symmetry, sparsity, and mathematically structured modeling approaches. His work integrates mathematical foundations, algorithm design, and physically motivated models across classical and quantum information processing.



Tharso Dominisini Fernandes received the B.Sc. degrees in Mathematics from the Federal University of Espírito Santo (UFES), Brazil, and in Computer Science from Fundação de Assistência e Educação (FAESA), Brazil, in 2005, and the M.Sc. and Ph.D. degrees in Computational Modeling from the National Laboratory for Scientific Computing (LNCC), Brazil, in 2008 and 2017, respectively. He is currently an Assistant Professor with the Department of Pure and Applied Mathematics

at the Federal University of Espírito Santo, Alegre, Brazil. His research interests include algebra, quantum computing, quantum walks, and quantum machine learning. He has authored and coauthored several journal and conference papers. He received the Howard E. Brandt Best Paper Award 2016 from *Quantum Information Processing* in 2017.